

Synthesis, Structures, and Properties of Two Isomeric Naphthodithiophenes and Their Methyl, Methylthio, and 2-Thienyl Derivatives; Application to Conductive Charge-Transfer Complexes and Low-Bandgap Polymers

Kazuo Takimiya,* Ken-ichi Kato, Yoshio Aso, Fumio Ogura, and Tetsuo Otsubo*

Department of Applied Chemistry, Graduate School of Engineering, Hiroshima University, Higashi-Hiroshima 739-8527

(Received February 6, 2002)

Two isomeric naphthodithiophenes (*syn*-NDT and *anti*-NDT), isoelectronic with pyrene, as well as their dimethyl, bis(methylthio), and di(2-thienyl) derivatives have been successfully synthesized as novel *peri*-fused heteroaromatics. Among them, the parent *syn*-NDT and the di(2-thienyl) derivative of *anti*-NDT were examined by X-ray crystallographic analyses, revealing that the molecular structures comprise fairly planar, but considerably strained skeletal rings, and their crystal structures are characterized by a herringbone arrangement of uniform stacking columns. The UV/vis spectra of these heteroaromatics show considerable red-shifts of the π–π^* transitions as compared to that of pyrene, making them chromogens ranging from yellow to purple. Cyclic voltammetry indicates that they have much stronger electron donating abilities than pyrene. Consequently, all of them, except for the methyl derivatives, can form highly conductive molecular complexes with iodine and DDQ. In addition, the electrochemical oxidation of the parent naphthodithiophenes and the di(2-thienyl) derivatives leads to the formation of conductive polymers, which show low HOMO–LUMO bandgaps upon undoping. In particular, both polymers of *syn*-NDT and *anti*-NDT have very low bandgaps of ca. 0.8 eV (77 kJ mol^{-1}).

Sulfur-containing aromatic compounds represent an interesting class of advanced materials for use in organic conductors,[1] electroluminescent devices,[2] electrochromic devices,[3] and field-effect transistors.[4] Since perylene (**1**) and pyrene (**2**) served as good electron donors for early conductive molecular complexes,[5] it has been naturally expected that more superior electron donors can be designed by sulfur incorporation into such *peri*-fused polynuclear aromatic compounds. As the first sulfur-containing compound isoelectronic with perylene, Wudl and co-workers in 1979 reported anthra[1,9-*bc*:5,10-*b′c′*]dithiophene (**3**), which was modified by the introduction of two thiophene rings.[6] Afterwards, our group reported a more elaborate variant, benzo[1,3-*cd*:4,6-*c′d′*]bis(thieno[2,3-*b*]thiophene) (**4**), tailored with four peripheral thiophenes.[7] Sulfur atoms incorporated serve to enhance the donor abilities, polarizability, and intermolecular interactions of such molecules.[8] Regarding similar isoelectronic variants of pyrene, on the other hand, little has been studied, although phenaleno[1,9-*bc*]thiophene (**5**) possessing a single thiophene ring was already reported in 1981, but with no detailed properties.[9] More intriguing are naphthodithiophenes, which have two regioisomers (*syn*-NDT **6** and *anti*-NDT **10**). The aromatic characters of these compounds are greatly reduced by introducing two thiophene rings into the skeleton. In particular, **10** no longer contains Kekulé benzene in the most contributing resonance structure. MNDO MO calculations predict that, relative to the frontier orbitals of pyrene, the HOMO energy levels of NDTs increase, while the LUMO levels decrease: pyrene, *E* (HOMO) −8.25 (−796) and *E* (LUMO) −1.01 eV (−97.5 kJ mol^{-1}); **6**,

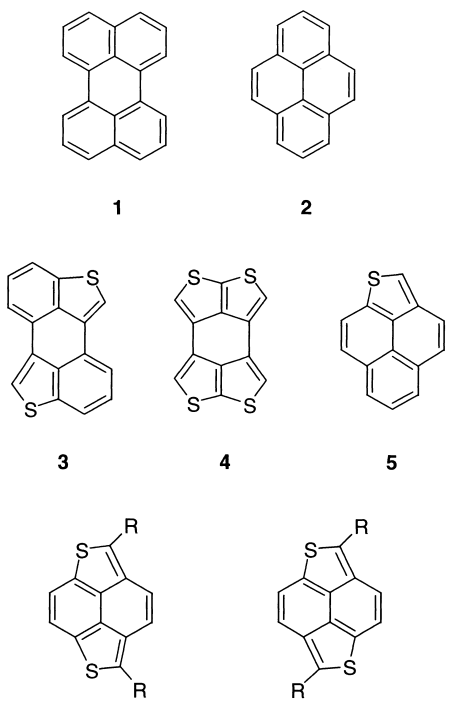

Chart 1.

−8.22 (−793) and −1.06 eV (−102 kJ mol^{-1}); **10**, −7.98 (−770) and −1.40 eV (−135 kJ mol^{-1}).[10] Furthermore, the 2-thienyl derivatives **9** and **13** strengthen this tendency: **9**, −7.86 (−758) and −1.62 eV (−156 kJ mol^{-1}); **13**, −7.66 (−739) and −1.82 eV (−176 kJ mol^{-1}). This indicates that the NDT compounds could behave as electroactive and photoactive materials (Chart 1).

Another noteworthy aspect of the NDT compounds is their application to low-bandgap polymers. The synthesis of low-bandgap polymers is a current challenge for constructing intrinsic organic metals.[11] Conjugated polyaromatics without doping usually have large bandgaps between the valence and conduction bands, owing to bond-length alternation. A principal guideline for reducing the bandgaps is to increase the contribution of the quinonoid resonance forms in the polymer structures to relax the bond-length alternation. Poly(isothianaphthene) (**14**) is the first molecule that has shown a low bandgap based on this guideline.[12] The extremely low bandgap (1.0 eV = 96.5 kJ mol^{-1}) of **14**, as compared to polythiophene (2.1 eV = 203 kJ mol^{-1}), indicates a good energetic balance between the aromatic form with *cata*-fused benzene rings and the quinonoid form with fused Kekulé benzene rings. Upon a similar consideration, the polymers (**15**–**18**) linked at the thiophene rings of **6**, **9**, **10**, and **13** are also expected to possess low bandgaps (Chart 2). In these cases, the quinonoid form, stabilized by an aromaticity gain of the central naphthalene ring instead of an aromaticity loss of two thiophene rings, can energetically balance with the aromatic form.

From the above two viewpoints, we have studied the NDT systems. In our early study for the synthesis of **6** and **10**, we examined an approach via transannular dehydrogenation reactions of [2.2](2,4)thiophenophane-1,8-dienes (**20** and **21**) as a key step, reminiscent of pyrene formation from [2.2]metacyclophane-1,9-diene (**19**) (Scheme 1).[13] When **20** was prepared by a conventional cyclophane synthetic method, it was spontaneously dehydrogenated to **6**.[14] However, the multi-step synthesis and low total yield of **6** made it difficult to study its properties in further detail. In addition, **21**, similarly obtained, allowed no formation of **10** under either thermal or photochemical conditions. These results have prompted us to develop practical synthetic methods of the two isomeric NDTs.[15] In this article, we report on the detailed synthesis, structures, donor properties, charge-transfer complexation, and polymerization of the parent compounds, **6** and **10**, as well as their methyl, methylthio, and 2-thienyl derivatives (**7**–**9** and **11**–**13**).

Results and Discussion

Synthesis. For a practical synthesis of **6**, we explored the benzannelation of benzo[1,2-*b*:4,3-*b*′]dithiophene derivatives, as shown in Scheme 2. A reductive self-coupling reaction of 4-methyl-2-thiophenecarbaldehyde (**22**),[16] mediated by low-valent titanium,[17] afforded *trans*-1,2-bis(4-methyl-2-thien-

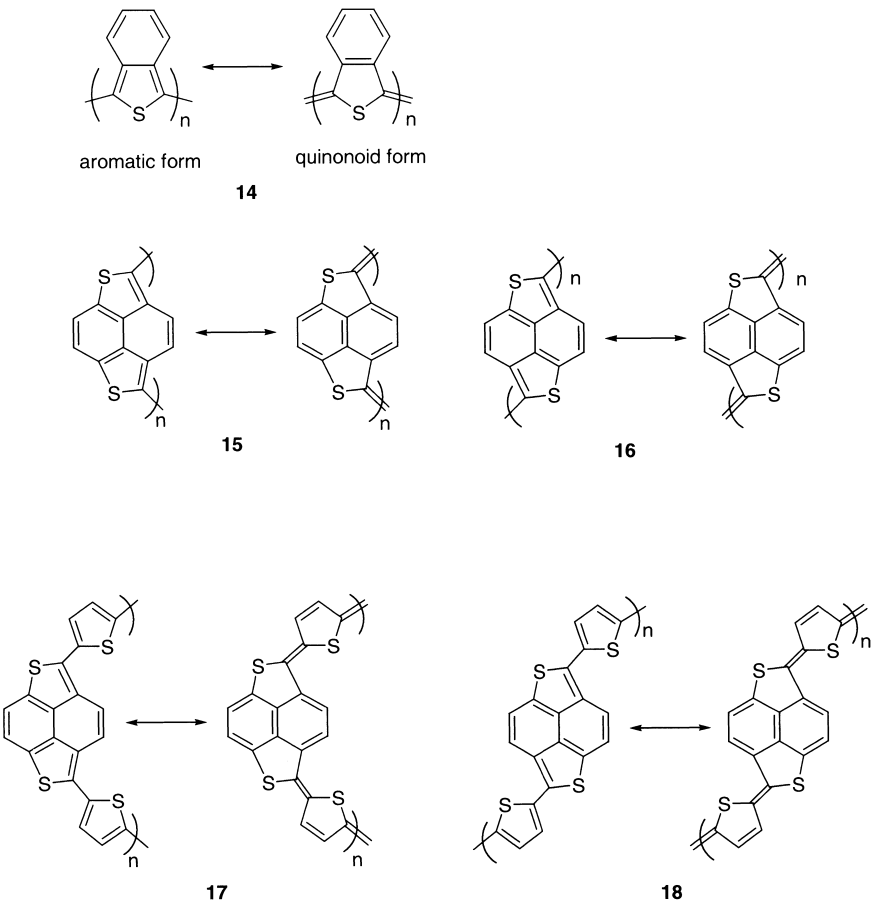

Chart 2.

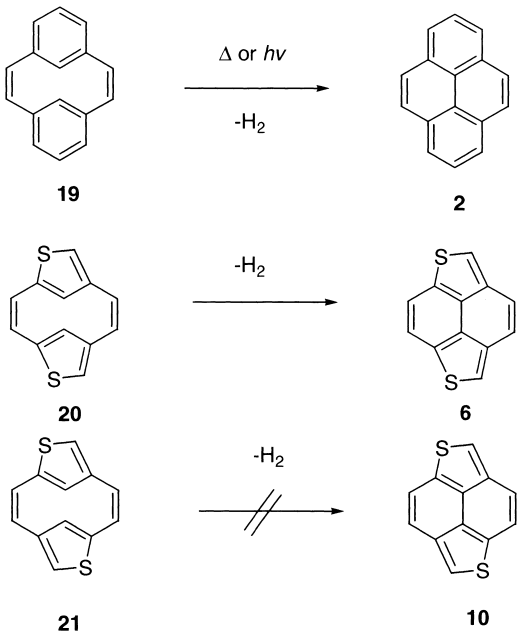

Scheme 1. Previous approach to naphthodithiophenes.

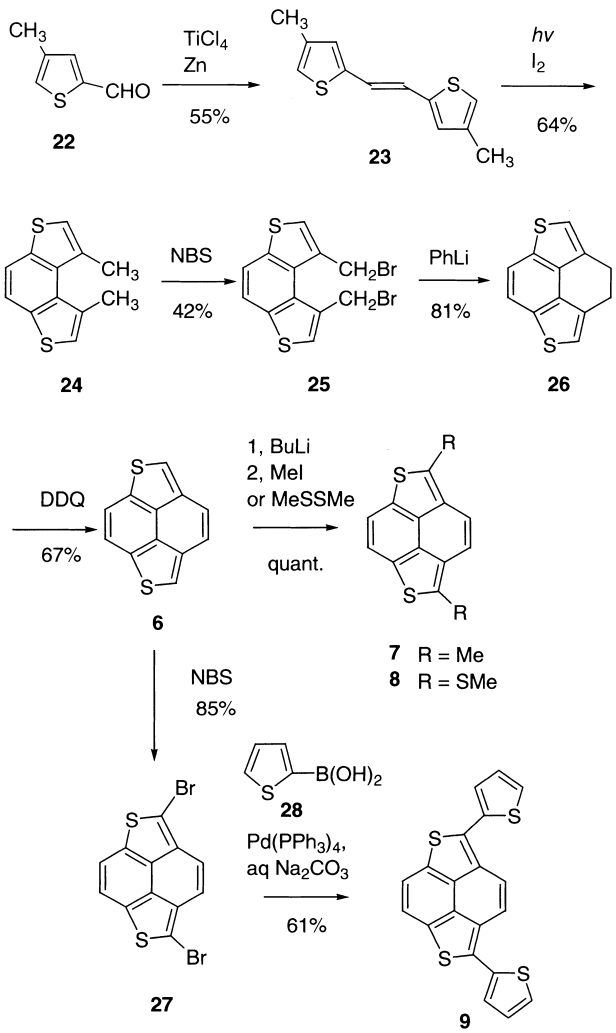

Scheme 2. Synthetic route of *syn*-naphthodithiophenes **6**–**9**.

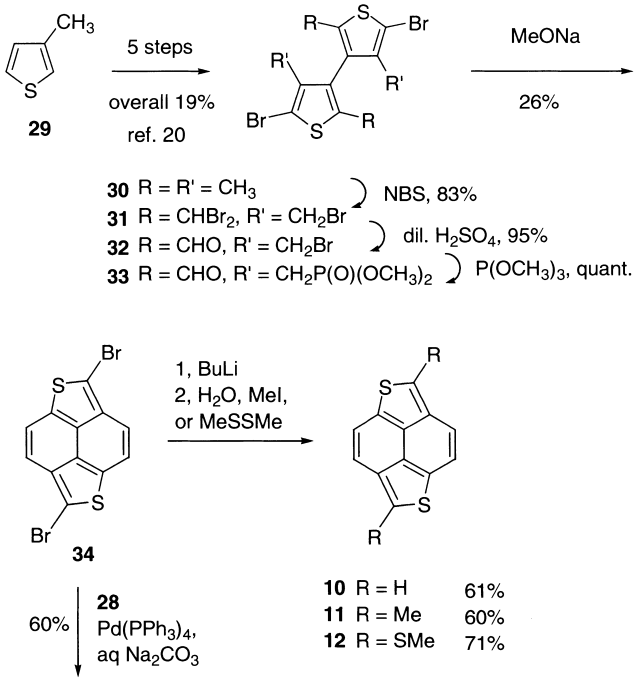

Scheme 3. Synthetic route of *anti*-naphthodithiophenes **10**–**13**.

yl)ethene (**23**) in 55% yield, which was then subjected to oxidative photocyclization[18] to give **24** in 64% yield. The radical bromination of **24** with *N*-bromosuccinimide (NBS) to the bis(bromomethyl) derivative **25** (42% yield), followed by Wurtz-type intramolecular C–C bond formation promoted by phenyllithium, gave 3,4-dihydronaphtho[1,8-*bc*:4,5-*b*′*c*′] dithiophene (**26**) in 81% yield. The dehydrogenation of **26** to **6** was performed with 2,3-dichloro-5,6-dicyano-1,4-benzoquinone (DDQ) in 67% yield. The large-scale preparation of **6** enabled us to study its derivatives **7**–**9**. Thus, the treatment of **6** with excess butyllithium, followed by methyl iodide and by dimethyl disulfide, gave 2,5-dimethyl derivative **7** and 2,5-bis(methylthio) derivative **8**, respectively, in quantitative yields. Alternatively, **6** with NBS was converted to the 2,5-dibromo derivative **27** (85%), which was subjected to Suzuki coupling with dihydroxy-2-thienylborane (**28**) to give the 2,5-di(2-thienyl) derivative **9** in 61% yield. Maradpour independently reported on the synthesis of the dimethyl derivative **7** via a different benzannelation route of a benzo[1,2-*b*:4,3-*b*′]dithiophene derivative.[19]

For the synthesis of center-symmetrical **10**, we examined the double benzannelation of 3,3′-bithiophene derivatives. As shown in Scheme 3, 5,5′-dibromo-2,2′,4,4′-tetramethyl-3,3′-

bithiophene (**30**), prepared in five steps from commercially available 3-methylthiophene (**29**) according to the literature,[20] was brominated with excess NBS to give 4,4′-bis(bromomethyl)-2,2′-bis(dibromomethyl)-5,5′-dibromo-3,3′-bithiophene (**31**) in 83% yield. The subsequent hydrolysis of **31** with dilute sulfuric acid in 1,4-dioxane gave the corresponding dialdehyde **32** in 95% yield, which was then converted into the phosphonate **33** in a quantitative yield by refluxing in neat trimethyl phosphite. An intramolecular double Wittig–Horner reaction of **33** using sodium methoxide as a base provided 2,6-dibromonaphto[1,8-*bc*:5,4-*b′c′*]dithiophene (**34**) in 26% yield. Finally, **34** was metallated with butyllithium and quenched with water to give **10** in 61% yield. Similarly, the methyl derivative **11** (60% yield) and the bis(methylthio) derivative **12** (71% yield) were prepared by treatments of the metallated species with excess methyl iodide and dimethyl disulfide, respectively. The di(2-thienyl) derivative **13** was also prepared by Suzuki coupling with dihydroxy-2-thienylborane (**28**) (60% yield). In contrast to the stable *syn*-isomer **6**, the *anti*-isomer **10** is very unstable either in solution or in the solid state, reflecting its greatly reduced aromatic structure with no Kekulé benzene ring. On the other hand, the derivatives **11**–**13** are relatively stable in the solid state, but tend to be more or less labile in solution.

Molecular and Crystal Structures. Single crystals of *syn*-NDT **6** and the di(2-thienyl) derivative of *anti*-NDT **13** were obtained by recrystallization from a chloroform–hexane mixed solvent, and their molecular and crystal structures were elucidated by X-ray crystallographic analyses. The molecular structures are demonstrated in Fig. 1, and the bond lengths and bond angles are summarized in Tables 1 and 2. Although the molecular structure of **6** is completely planar, the skeletal rings are fairly deformed. The most strained part of the molecule is the six-membered ring defined by C8, C9, C10, C11, C13, and C14, where the bond lengths of C8–C9 and C10–C11 are much longer (1.45–1.46 Å) than the normal C–C length (1.39 Å) of benzene, while the bond length of C9–C10 is shorter (1.347 Å). In addition, the bond angles in the ring greatly deviate from 120°, ranging from 115.6° for the C10–C11–C13 to

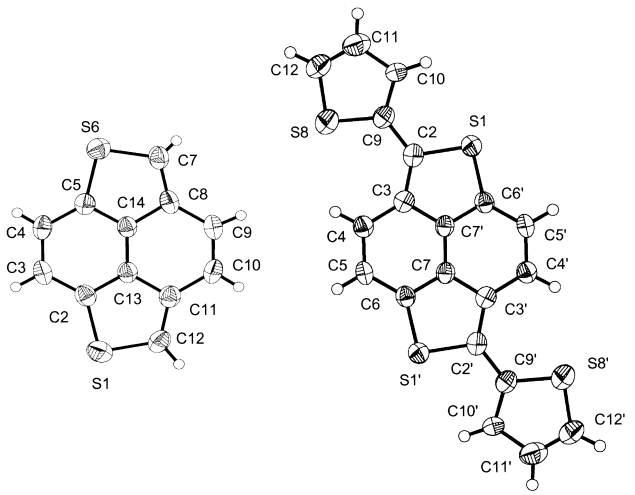

Fig. 1. (a) ORTEP drawing of **6** and (b) ORTEP drawing of **13**.

Table 1. Bond Lengths and Bond Angles of **6**

Bond length/Å		Bond angle/°	
S1–C2	1.727(4)	C2–S1–C12	94.0(2)
S1–C12	1.731(4)	S1–C2–C13	107.7(3)
C2–C3	1.410(5)	C3–C2–C13	118.6(4)
C2–C13	1.387(5)	C2–C3–C4	120.5(4)
C3–C4	1.373(6)	C3–C4–C5	120.3(4)
C4–C5	1.409(5)	C4–C5–C14	119.0(4)
C5–S6	1.752(4)	S6–C5–C14	107.8(3)
C5–C14	1.387(5)	C5–S6–C7	92.9(2)
S6–C7	1.724(4)	S6–C7–C8	112.7(3)
C7–C8	1.396(7)	C7–C8–C14	109.7(4)
C8–C9	1.454(6)	C9–C8–C14	116.1(4)
C8–C14	1.419(5)	C8–C9–C10	122.1(4)
C9–C10	1.347(7)	C9–C10–C11	121.9(4)
C10–C11	1.466(6)	C10–C11–C13	115.6(4)
C11–C12	1.386(6)	C12–C11–C13	110.0(3)
C11–C13	1.426(5)	C11–C12–S1	111.5(3)
C13–C14	1.380(6)	C11–C13–C14	122.1(3)
		C8–C14–C13	122.1(4)
		C5–C14–C13	120.6(3)
		C2–C13–C14	121.0(3)
		C2–C13–C11	116.9(4)
		C5–C14–C8	117.3(4)

Table 2. Bond Lengths and Angles of **13**

Bond length/Å		Bond angle/°	
S1–C2	1.762(7)	C2–S1–C6	93.6(3)
S1–C6′	1.735(7)	C9–S8–C12	92.7(4)
S8–C9	1.711(7)	S1–C2–C3	110.6(5)
S8–C12	1.682(8)	S1–C2–C9	118.5(5)
C2–C3	1.391(9)	C3–C2–C9	130.9(6)
C2–C9	1.447(9)	C2–C3–C4	133.3(6)
C3–C4	1.449(9)	C2–C3–C7′	110.2(6)
C3–C7′	1.426(9)	C4–C3–C7′	116.5(6)
C4–C5	1.373(9)	C3–C4–C5	120.6(6)
C5–C6	1.422(9)	C4–C5–C6	121.2(6)
C6–C7	1.376(9)	S1′–C6–C5	132.7(5)
C7–C7′	1.40(1)	S1′–C6–C7	107.8(5)
C9–C10	1.417(9)	C5–C6–C7	119.5(6)
C10–C11	1.43(1)	C3′–C7–C6	117.9(6)
C11–C12	1.32(1)	C3′–C7–C7′	121.8(7)
		C6–C7–C7′	120.3(7)
		S8–C9–C2	122.3(5)
		S8–C9–C10	111.4(5)
		C2–C9–C10	126.3(6)
		C9–C10–C11	108.2(6)
		C10–C11–C12	115.8(7)
		S8–C12–C11	111.9(6)

122.1° for the C11–C13–C14, although the other six-membered ring, defined by C2, C3, C4, C5, C14, and C13, is less deformed. On the other hand, the fused thiophene rings keep nearly the same skeletons as normal thiophene.[21] These bond-length alternations and bond angle deviations properly reflect the most contributing resonance structure of **6**. The molecular structure of **13** is also nearly planar, even including the two additional thiophene rings. Although this molecule is also severely strained, the principal strain is distributed equally over the

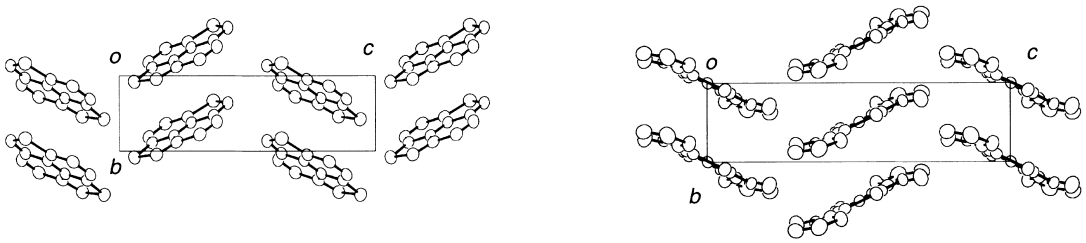

Fig. 2. (a) Crystal structure of **6** and (b) crystal structure of **13**.

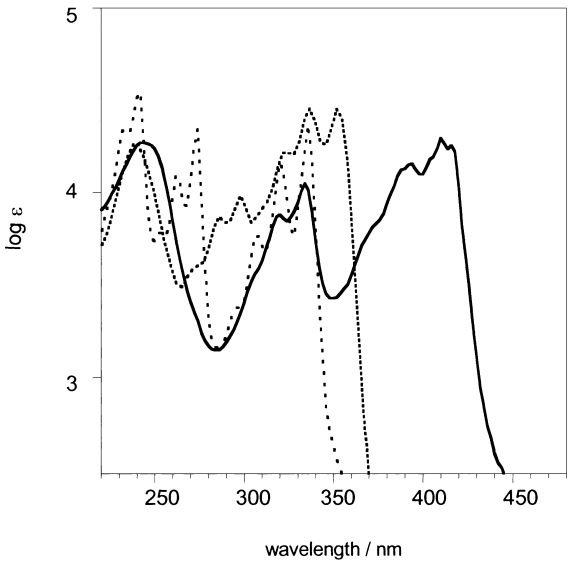

Fig. 3. Electronic absorption spectra of **6** (dotted line) and **10** (solid line) together with pyrene (dashed line) in THF.

two central six-membered rings.

The crystal structure of pyrene is characterized by a herringbone arrangement of molecular pairs loosely stacked with a center of symmetry, and there are no direct π–π overlaps among the pairs.[22] In contrast, in the crystal structures of **6** and **13**, the molecules are stacked face-to-face with van der Waals contacts to form uniform columns, which are packed in a herringbone pattern (Fig. 2). Among the neighboring columns, there are weak nonbonded S–S contacts of the skeletal thiophene rings of **6** (3.76 Å). On the other hand, in **13**, the skeletal thiophene ring is rather close to the thienyl group of the neighboring molecule with an S–S distance of 3.78 Å.

Electronic Spectra. The reduced aromatic characters of the NDT compounds are reflected in their electronic absorption spectra; **6** shows three strong bands at 239, 299, and 353 nm in THF, and **10** at 245, 334, and 411 nm, as demonstrated in Fig. 3. The two longer wavelength bands with fine structures are considerably red-shifted as compared to the corresponding bands (273 and 336 nm) of pyrene. In particular, the longest wavelength band of **10** exceeds 400 nm, indicating a small energy gap between the HOMO and LUMO levels. The methyl, methylthio, and 2-thienyl derivatives also exhibit similar absorption bands with further large red-shifts due to the substituent effects, as summarized in Table 3. In accordance with these different absorption maxima, the NDT compounds are deeply colored, ranging from yellow to purple. In the fluorescence spectra, the emission bands are also red-shifted, in agreement with the shifts of the absorption bands.

Table 3. Electronic Absorption Maxima,[a] Emission Maxima,[a] and Oxidation Potentials[b]

Compd	Appearance	λ_{abs}/nm (log ε)	λ_{emis}/nm	E_{pa}[c]/V	$E_{1/2}$[d]/V
6	Pale yellow needles	239 (4.25), 287 (3.85), 299 (3.98), 336 (4.49), 353 (4.46)	380	1.01[e]	
7	Yellow needles	242 (4.27), 287 (3.91), 299 (4.06), 348 (4.39), 364 (4.37)	380	0.92	0.84
8	Yellow needles	250 (4.13), 309 (3.92), 320 (3.93), 387 (4.53)	432	0.77	0.71, 0.97
9	Orange needles	230 (4.30), 346 (4.02), 444 (4.53)	493	0.89[e]	
10	Yellow fine crystals	245 (4.28), 320 (3.88), 334 (4.04), 394 (4.15) 411 (4.29), 417 (4.25)	427	0.93[e]	
11	Ocherous powder	247 (4.36), 319 (3.88), 335 (4.05), 414 (4.21), 432 (4.37), 439 (4.33)	450	0.63[e]	
12	Ocherous powder	262 (4.26), 334 (3.89), 349 (4.01), 448 (4.42)	510	0.58	0.53, 0.91
13	Purple needles	287 (4.33), 345 (3.87), 519 (4.57)	564	0.62[e]	
2 (pyrene)	Pale yellow prisms	232 (4.34), 241 (4.57), 262 (4.09), 273 (4.35), 320 (4.15), 336 (4.36)	373	1.35[e]	

a) Measured in tetrahydrofuran. b) Cyclic voltammetry was recorded at 100 mVs^{-1} scan rate with Pt working and counter electrodes and Ag/AgCl reference electrode in 10^{-3} mol dm^{-3} benzonitrile solution containing 0.1 mol dm^{-3} tetrabutylammonium perchlorate as supporting electrolyte. c) First oxidation peak potential. d) Half-wave oxidation potential. e) Irreversible wave.

Electrochemistry. In cyclic voltammetry, the parent compounds, **6** and **10**, show irreversible oxidation waves at +1.01 V and +0.93 V, respectively, vs Ag/AgCl reference electrode, which are much lower than that of pyrene (+1.35 V). This evidently indicates increasing electron donating abilities of the NDT compounds. The lower oxidation potential of **10** relative to **6** is in accordance with the MO calculation. The repeated redox cycles of **6** and **10** show a gradual growth of a new peak at approximately 0.5 V, as demonstrated for **6** in Fig. 4. This result means that the α-positions of the thiophene moieties in **6** and **10** are susceptible to electrochemically oxidative coupling on the working electrode, as well known for thiophene systems. The prolonged potentiostatic oxidation at 1.2 V results in the formation of insoluble black polymers, which exhibit conductivities of 1.6×10^{-2} S cm^{-1} for poly-**6** (**15**) and 2.3×10^{-4} S cm^{-1} for poly-**10** (**16**).[23]

The methyl, methylthio, and 2-thienyl derivatives show much lower oxidation waves than those of the parent compounds owing to the substituent effects (see Table 3). In particular, the methylthio derivatives, **8** and **12**, demonstrate not only the marked lowering of the first oxidation waves, but also the appearance of the second oxidation waves. This indicates that the conjugation effect of the methylthio group is very effective in enhancing the electron-donating ability of this system. In addition, the methyl and methylthio derivatives, except for unstable **11**, show reversible oxidation waves owing to a masking of the reactive sites for electropolymerization. On the other hand, the 2-thienyl derivatives, **9** and **13**, like the parent ones, are also electrochemically reactive, giving black conductive polymers, poly-**9** (**17**) 5.3×10^{-3} S cm^{-1}and poly-**13** (**18**) 5.3×10^{-2} S cm^{-1}.[23]

Molecular Complexes. Since all of the new compounds have stronger electron-donating abilities than pyrene, they can more readily form molecular complexes with iodine and DDQ, as summarized in Table 4. The iodine complexes of the parent NDTs, **6** and **10**, exhibit high conductivity of 0.92 and 0.20 S cm^{-1}, respectively, measured on a compressed pellet sample at room temperature. These values exceed the reported conductivity for the pyrene–iodine complex (0.013 S cm^{-1}).[5c,d] The DDQ complexes are also conductive, **6**·DDQ 2.1 S cm^{-1} and **10**·DDQ 0.08 S cm^{-1}, being in sharp contrast to the insulating pyrene·DDQ complex (10^{-13} S cm^{-1}).[24] These results evidently demonstrate the successful molecular design of the NDT systems for isoelectronic heteroaromatics of pyrene. Although the crystal structures of these complexes have not yet been disclosed, it may be speculated that the nonbonded S–S interactions of the incorporated sulfur contribute to the enhancement of the conductivities.

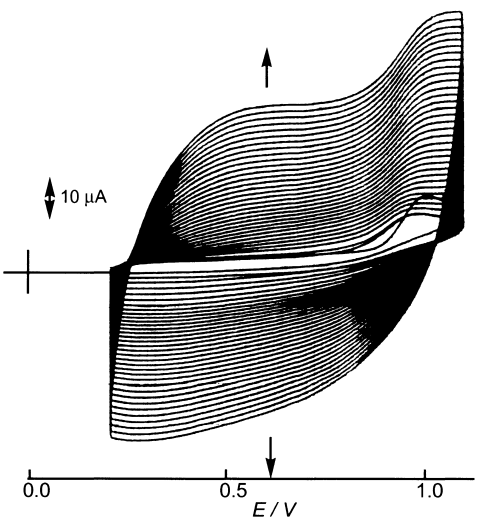

Fig. 4. Repetitive cyclic voltammetric scanning (100 mV s^{-1}) of **6** in benzonitrile containing 0.1 M tetrabutylammonium perchlorate.

The iodine and DDQ complexes of the methyl derivatives, **7** and **11**, are hardly conductive (< 10^{-4} S cm^{-1}). The attached methyl groups may sterically hinder the nonbonded S–S interactions of the naphthodithiophene core. In contrast, those of the methylthio and 2-thienyl derivatives, except for the **12**·DDQ complex, show high conductivities in the range of 10^{0}–10^{-2} S cm^{-1}. The sulfur atoms of the methylthio and 2-thienyl groups may also participate in the molecular interactions. The electrochemical as well as thermal stabilities of the methylthio derivatives, **8** and **12**, allowed for the formation of their radical cation salts by a conventional electrocrystallization method. The resulting BF_4^-, ClO_4^-, and PF_6^- salts are, however, less conductive than the iodine and DDQ complexes. The low conductivities (10^{-5}–10^{-6} S cm^{-1}) of these salts are ascribed to the 1:1 composition ratio, that is, complete charge transfer leading to Mott-Hubbard type insulators.[25] An exceptional case is the triiodide salt of **8** with 3:4 stoichiometry, which is supposed to be essentially the same as the above-mentioned powder sample obtained by mixing **8** and iodine. The single crystalline sample shows a very high conductivity of 27 S cm^{-1} at room temperature, but, regarding the temperature dependence, it is semiconductive with a relatively small activation energy (0.025 eV).

Low-Bandgap Polymers. Since the research of low-bandgap polymers was triggered off by the appearrance of poly(isothianaphthene) (**14**),[12] a number of conductive polymers with bandgaps below 1 eV have been developed up to now not only by the same strategy of increasing the contribution of the quinonoid resonance form to the ground state as **14**,[26] but also by a charge-transfer mixing strategy of alternately introducing donor and acceptor units in a polymer chain.[27] As already mentioned, the parent naphthodithiophenes, **6** and **10**, are electrochemically reactive to readily effect polymerization under the cyclovoltammetric conditions. Because the electrochemical and optical properties of the resulting poly-**6** and poly-**10** are very similar to each other, only those of poly-**10** are discussed, as follows. The cyclic voltammogram of poly-**10** deposited on a Pt disk electrode by anodic oxidation is shown in Fig. 5, demonstrating that the polymers are highly amphoteric ($E^{ox}_{1/2}$ +0.46 V and $E^{red}_{1/2}$ −1.35 V vs Ag/AgCl). The difference between the thresholds for the oxidation wave (*p*-doping) and for reduction wave (*n*-doping) is fairly smaller than 1.0 V, implying that the polymer actually has a very low bandgap. The electronic absorption spectra of poly-**10**, recorded at various cell potentials by using the film deposited on an indium tin oxide (ITO) glass electrode, are shown in Fig. 6. The oxidized film shows a polaronic (or bipolaronic) band cen-

Table 4. Charge-Transfer Complexes and Radical Cation Salts

Complex	Method[a]	D:A	Appearance	Dp/°C	Found(Calcd)[b]/%			σ[c]/S cm^{-1}
					C	H	N	
6·I_3	A	2:1	Black powder	> 300	36.69	1.69	0	0.92
					(35.62	1.49	0)	
6·DDQ	A	2:1	Black powder	> 300	58.45	1.83	3.32	2.1
					(58.63	1.84	4.27)	
7·I_3	A	3:1	Dark green powder	180	45.56	2.50	0	3.6×10^{-9}
					(45.54	2.73	0)	
7·DDQ	A	1:2	Black powder	> 300	52.18	1.71	7.07	1.2×10^{-8}
					(51.75	1.45	8.04)	
8·I_3	A	3:4	Dark green powder	128	20.65	1.26	0	1.3
					(20.66	1.24	0)	
8·I_3	B	3:4	Dark green needles	90	21.08	1.44	0	27[d]
					(20.66	1.24	0)	
8·DDQ	A	1:1	Black powder	156	49.36	1.81	5.58	5.5×10^{-2}
					(49.53	1.89	5.27)	
8·BF_4	B	1:1	Black fine crystals	192	42.93	2.39	0	1.1×10^{-5}
					(42.76	2.56	0)	
8·ClO_4	B	1:1	Black fine crystals	181	41.21	2.43	0	1.6×10^{-6}
					(41.43	2.48	0)	
8·PF_6	B	1:1	Black fine crystals	175	37.28	2.21	0	3.6×10^{-7}
					(37.25	2.23	0)	
9·I_3	A	1:1	Black powder	> 300	31.34	1.60	0	6.5
					(31.64	1.33	0)	
9·DDQ	A	1:1	Black powder	> 300	56.03	1.92	3.94	9.3
					(55.54	1.65	4.62)	
10·I_3	A	5:1	Black powder	> 300	48.92	2.11	0	0.2
					(49.63	2.08	0)	
10·DDQ	A	5:2	Black powder	> 300	59.65	1.75	2.86	8.0×10^{-2}
					(59.84	1.96	3.67)	
11·I_3	A	1:1	Black powder	> 300	45.16	2.78	0	5.4×10^{-4}
					(45.53	2.73	0)	
11·DDQ	A	3:1	Black powder	> 300	62.29	2.63	2.35	1.2×10^{-8}
					(62.96	3.14	2.93)	
12·I_3	A	3:2	Black powder	230	30.58	1.43	0	4.4×10^{-2}
					(30.01	1.79	0)	
12·DDQ	A	1:1	Black powder	235	49.30	1.85	5.25	3.2×10^{-4}
					(49.53	1.89	5.27)	
12·BF_4	B	1:1	Black powder	196	42.98	2.48	0	2.6×10^{-6}
					(42.76	2.56	0)	
12·ClO_4	B	1:1	Black powder	188	41.73	2.46	0	1.9×10^{-6}
					(41.43	2.48	0)	
13·I_3	A	1:1	Dark green powder	> 300	32.57	1.34	0	10.0
					(31.64	1.33	0)	
13·DDQ	A	1:1	Black powder	> 300	56.30	1.85	3.70	9.0
					(55.54	1.65	4.62)	

a) Method A: direct mixing of the acetonitrile solutions of donor and acceptor, and Method B: electrocrystallization in THF or acetonitrile. b) Calculated from stoichiometry indicated for each complex. c) Measured on a compressed pellet with a two- or four-probe method at room temperature unless otherwise stated. d) Measured on a single crystal with a four-probe method at room temperature.

tered at 1400 nm (0.88 eV = 84.9 kJ mol^{-1}). When it is dedoped at -0.2 V to the neutral film, an absorption band assignable to π–π^* transition is observed at 900 nm (1.37 eV= 132 kJ mol^{-1}). The bandgap of poly-**10** is estimated to be 0.86 eV (83.0 kJ mol^{-1}) from the on-set (1500 nm) of π–π^* absorption. In a similar optical measurement, the bandgap of poly-**6** was determined to be 0.83 eV (80.1 kJ mol^{-1}). These values are much smaller than the bandgap (1.0 eV = 96.5 kJ mol^{-1}) of poly(isothianaphthene) (**14**). Electropolymerization of the 2-thienyl derivatives, **9** and **13**, also provide similar polymers, which, however, have much higher bandgaps: poly-**9** 1.65 eV (159 kJ mol^{-1}) and poly-**13** 1.46 eV (141 kJ mol^{-1}). Presumably, the thienyl conjugation interferes with the relaxation of the bond-length alternation.

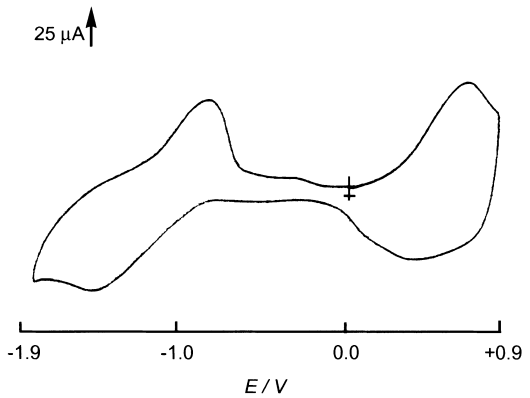

Fig. 5. Cyclic voltammogram of poly-**10** deposited on a Pt disk electrode recorded at a scan rate of 100 $mV\,s^{-1}$ in acetonitrile containing 0.1 M tetrabutylammonium perchlorate with Ag/AgCl reference electrode.

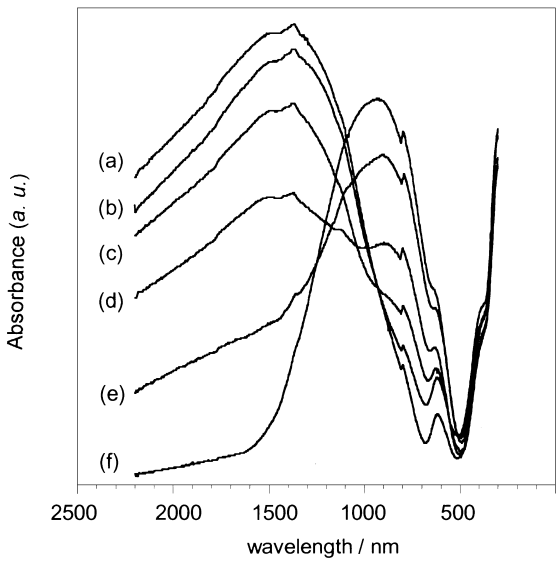

Fig. 6. UV-vis-NIR spectra of poly-**10** film deposited on an ITO electrode under variable cell potentials: (a) +0.8 V, (b) +0.6 V, (c) +0.4 V, (d) +0.2 V, (e) 0.0 V, and (f) −0.2 V vs Ag/AgCl reference electrode in acetonitrile containing 0.1 M tetrabutylammonium perchlorate.

Conclusions

According to the strategy of heteroatom-incorporation into aromatic hydrocarbons for developing new advanced materials, the two isomeric naphthodithiophenes, **6** and **10**, isoelectronic with pyrene, as well as the methyl, methylthio, and 2-thienyl derivatives have been successfully synthesized. As a result of the elevation of HOMO levels and the depression of LUMO levels, these NDT compounds are chromogens that can widely vary from yellow to purple, depending on the isomeric types and substituent groups. In addition, they have much stronger electron-donating abilities than pyrene, accordingly forming highly conductive complexes with iodine and DDQ. Among them, the parent compounds, **6** and **10**, and the 2-thienyl derivatives, **9** and **13**, can electrochemically polymerize at the α-thiophene positions, giving conductive polymers, which behave as low-bandgap polymers in the neutral states. In particular, the poly-**6** and pol-**10** have very low bandgaps of ca. 0.8 eV (77 kJ mol^{-1}), which are among the lowest for conductive polymers known up to the present.

Experimental

General. The melting points are uncorrected. All of the chemicals and solvents were of reagent grade. ^{1}H NMR spectra were recorded on a Hitachi R-1200 (60 MHz), a Bruker AMX-400wb (400 MHz), or a JEOL Lambda 400 (400 MHz) spectrometer using deuteriochloroform as a solvent and tetramethylsilane as an internal standard, unless otherwise stated. ^{13}C NMR spectra were recorded on a Bruker AMX-400wb (100 MHz) or a JEOL Lambda 400 (100 MHz) spectrometer using deuteriochloroform as a solvent and tetramethylsilane as an internal standard. IR spectra were taken on a Hitachi 260-30 or a Shimadzu FTIR 8100 spectrophotometer with a KBr disk method. MS spectra were measured at 70 eV on a Shimadzu QP-1000A or Shimadzu QP-2000 spectrometer using a direct insertion technique. High-resolution mass spectra were taken at 70 eV on a Hitachi MS 80B spectrometer using a direct insertion technique. UV-vis-NIR spectra were recorded on a Shimadzu UV-3100 spectrophotometer. Cyclic voltammetry was carried out on a Hokuto Denko HA-301 potentiostat and a Hokuto Denko HB-104 function generator. Variable temperature-dependent conductivity measurements were carried out with a Fuso Multi-Channel 4-Terminal Conductometer HECS 994. Preparative gel permeation chromatography (GPC) was performed on a Japan Analytical Industry LC-908 equipped with a JAI-GEL 1H, 2H column assembly. 4-Methyl-2-thiophenecarbaldehyde (**22**)[16] and 5,5′-dibromo-2,2′,4,4′-tetramethyl-3,3′-bithienyl (**30**)[20] were prepared from commercially available 3-methylthiophene according to the reported procedures.

***trans*-1,2-Bis(4-methyl-2-thienyl)ethene (23).** 4-Methyl-2-thiophenecarbaldehyde (**22**, 31.5 g, 0.25 mol) was added to a yellow suspension of $TiCl_4$ in THF, which was prepared by the slow addition of $TiCl_4$ (74.4 g, 0.39 mol) to THF (800 mL) with ice-cooling.[17] After the mixture was cooled with an ice-salt bath, zinc powder (50 g) was added by portions with care. The color of the suspension turned black, and the mixture was warmed to room temperature and refluxed for 9 h. After cooling, the mixture was poured onto ice (ca. 1000 g), hydrolyzed with saturated aqueous $NaHCO_3$ (500 mL), and extracted with CH_2Cl_2 (200 mL × 3). The extract was dried ($MgSO_4$) and concentrated. The crude residue was passed through a short column of silica gel using hexane as an eluent and recrystallized from hexane to afford colorless prisms of **23** (15.1 g, 55%): mp 132 °C; ^{1}H NMR (60 MHz) δ 2.22 (d, J = 0.8 Hz, 6H, CH_3), 6.75 (br s, 2H, ArH), 6.84 (s, 2H, ArH), and 6.95 (s, 2H, olefin); ^{13}C NMR δ 15.63, 119.54, 121.17, 128.15, 138.14, and 142.09; MS *m/z* 220 (M^+). Found: C, 65.40; H, 5.42%. Calcd for $C_{12}H_{12}S_2$: C, 65.41; H, 5.49%.

1,8-Dimethylbenzo[1,2-*b*:4,3-*b*′]dithiophene (24). A benzene solution (350 mL) of **23** (1.1 g, 0.05 mol) was irradiated by a high-pressure mercury lamp with bubbling dry air at 20 °C. The progress of the reaction was checked by ^{1}H NMR, until the spectral signals of **23** disappeared. The solution was washed with aqueous $NaHSO_3$ (300 mL) and water (200 mL), dried ($MgSO_4$), and concentrated in vacuo. The crude product was purified by silica-gel chromatography using hexane as an eluent. Recrystallization from hexane–benzene gave colorless prisms of **24** (0.7 g, 64%): mp 114–116.5 °C; ^{1}H NMR (400 MHz) δ 2.79 (s, 6H,

CH_3), 7.16 (s, 2H, ArH), and 7.73 (s, 2H, ArH); ^{13}C NMR δ 21.63, 119.35, 123.56, 133.02, 134.31, and 139.59; MS *m/z* 218 (M^+). Found: C, 65.88; H, 4.58%. Calcd for $C_{12}H_{10}S_2$: C, 66.01; H, 4.62%.

1,8-Bis(bromomethyl)benzo[1,2-*b*:4,3-*b′*]dithiophene (25). To a refluxing mixture of NBS (1.06 g, 5.95 mmol) and benzoyl peroxide (10 mg) in carbon tetrachloride (25 mL) was added **24** (545 mg, 2.5 mmol); the mixture was refluxed for 30 min. After cooling, the solvent was evaporated and the resulting residue was washed with hot water to leave crude **25**. Recrystallization from chloroform gave colorless needles (394 mg, 42%): mp 130–132 °C (melt with decomposition); ^{1}H NMR (400 MHz) δ 5.36 (s, 4H, CH_2), 7.72 (s, 2H, ArH), and 7.83 (s, 2H, ArH); ^{13}C NMR δ 32.41, 120.31, 129.50, 131.51, 133.73, and 140.75; MS *m/z* 374, 376, and 378 (M^+). Found: C, 38.45; H, 2.22%. Calcd for $C_{12}H_8S_2Br_2$: C, 38.32; H, 2.14%.

3,4-Dihydronaphtho[1,8-*bc*:4,5-*b′c′*]dithiophene (26). To a solution of **25** (376 mg, 1 mmol) in THF (15 mL) was added 1.2 mL of phenyllithium solution (1.2 M in cyclohexane, 1 M = 1 mol dm^{-3}) under a nitrogen atmosphere. After additional stirring for 30 min at RT, the mixture was poured onto ice (30 g), acidified with 1 M hydrochloric acid (15 mL), and extracted with dichloromethane (15 mL × 3). The extract was washed with water, dried ($MgSO_4$), and concentrated under reduced pressure. Silica-gel chromatography eluted with hexane afforded **26** (176 mg, 81%). Recrystallization from hexane–benzene gave colorless prisms: mp 109–109.5 °C: ^{1}H NMR (400 MHz) δ 3.17 (s, 4H, CH_2), 7.10 (s, 2H, ArH), and 7.72 (s, 2H, ArH); ^{13}C NMR δ 24.12, 118.37, and 119.74; MS *m/z* 216 (M^+). Found: C, 66.60; H, 3.73%. Calcd for $C_{12}H_8S_2$: C, 66.63; H, 3.73%.

Naphtho[1,8-*bc*:4,5-*b′c′*]dithiophene (6). Under a nitrogen atmosphere, a mixture of **26** (80 mg, 0.37 mmol) and DDQ (83.7 mg, 0.37 mmol) in toluene (10 mL) was refluxed for 4 h. After cooling, the resulting black precipitate was filtered off, and the filtrate was washed successively with a 10% aq NaOH solution (20 mL), water (20 mL), and brine (20 mL), and dried ($MgSO_4$). Evaporation of the solvent under reduced pressure afforded a brown solid (73 mg), which was purified with GPC and then recrystallized from chloroform–hexane to give pale-yellow needles of **6** (47 mg, 67%): mp 187–188 °C (melt with decomposition); ^{1}H NMR (400 MHz) δ 7.29 (s, 2H), 7.52 (s, 2H), and 7.94 (s, 2H); ^{13}C NMR δ 119.21, 119.54, and 122.30; MS *m/z* 214 (M^+). Found: C, 67.23; H, 3.03%. Calcd for $C_{12}H_6S_2$: C, 67.25; H, 2.82%.

2,5-Dimethylnaphtho[1,8-*bc*:4,5-*b′c′*]dithiophene (7). To a mixture of butyllithium (1.6 M solution in hexane, 1.45 mL, 2.3 mmol) and TMEDA (0.92 mL) in THF (8 mL) was added a solution of **6** (130 mg, 0.61 mmol) in THF (10 mL) at −78 °C. The mixture was stirred for 1.5 h at −30 °C, then cooled to −78 °C; methyl iodide (0.7 mL) was then added. The resulting mixture was allowed to warm to room temperature, and was further stirred overnight. After a treatment with 1 M hydrochloric acid (10 mL), the mixture was extracted with benzene (10 mL × 3). The extract was dried ($MgSO_4$) and concentrated in vacuo to afford light-brown crystals of **7** (146 mg, quant.). The crude product was purified by column chromatography on silica gel (eluted with benzene–hexane 1:1), followed by recrystallization from hexane to give pure **7** as yellow needles: mp 96–97 °C (lit.[19] mp 98–98.5 °C); ^{1}H NMR (400 MHz) δ 2.74 (s, 3H, CH_3), 7.07 (s, 2H, ArH), and 7.68 (s, 2H, ArH); ^{13}C NMR δ 13.49, 118.09, 119.82, 127.49, 130.64, 133.57, and 135.11; MS *m/z* 242 (M^+). Found: C, 69.35; H, 4.16%. Calcd for $C_{14}H_{10}S_2$: C, 69.38; H, 4.16%.

2,5-Bis(methylthio)naphtho[1,8-*bc*:4,5-*b′c′*]dithiophene (8). To a solution of the dilithiated **6**, prepared as described above, excess dimethyl disulfide was added. The mixture was stirred for 1.5 h at −30 °C, and then worked up in a similar manner as described for **7**: quantitative yield; yellow needles from hexane; mp 80 °C; ^{1}H NMR (400 MHz) δ 2.61 (s, 3H, CH_3), 7.37 (s, 2H, ArH), and 7.76 (s, 2H, ArH); ^{13}C NMR δ 22.20, 119.04, 121.20, 132.47, 132.97, 133.46, and 134.14; MS *m/z* 306 (M^+). Found: C, 54.82; H, 3.25%. Calcd for $C_{14}H_{10}S_4$: C, 54.86 ; H, 3.29%.

2,5-Dibromonaphtho[1,8-*bc*:4,5-*b′c′*]dithiophene (27). After a solution of **6** (45 mg, 0.21 mmol) and NBS (82 mg, 0.46 mmol) in 1:1 acetic acid–chloroform (10 mL) was stirred at RT for 2 h, the resulting solid was filtered off. The filtrate was washed successively with aq. sat. $NaHCO_3$ and water, dried ($MgSO_4$), and concentrated in vacuo. The residue was purified by column chromatography on silica gel with 1:1 benzene–hexane, followed by recrystallization from benzene–hexane to give **27** as orange crystals (66 mg, 85%): mp 145 °C (decomposition); ^{1}H NMR (400 MHz) δ 7.16 (s, 2H, ArH), and 7.71 (s, 2H, ArH); ^{13}C NMR δ 109.92, 118.74, 121.42, 130.26, 132.50, and 132.79; MS *m/z* 370, 372, and 374 (M^+). Found: C, 38.73; H, 1.19%. Calcd for $C_{12}H_4S_2Br_2$: C, 38.73; H, 1.07%.

2,5-Di(2-thienyl)naphtho[1,8-*bc*:4,5-*b′c′*]dithiophene (9). After a solution of **27** (107 mg, 0.287 mmol) and tetrakis(triphenylphosphine)palladium (131 mg, 0.144 mmol) in THF (20 mL) was stirred at RT for 10 h, 1 M aq Na_2CO_3 (18 mL) and dihydroxy-2-thienylborane (**28**) (293 mg, 2.30 mmol) were added. The mixture was stirred at RT for 2 h, and washed with water, dried ($MgSO_4$), and concentrated in vacuo. The residue was purified by column chromatography on silica gel with dichloromethane–hexane (2:1, v/v), followed by recrystallization from benzene–hexane to give **9** as orange needles (67 mg, 61%): mp 232–234 °C; ^{1}H NMR (400 MHz) δ 7.11 (dd, J = 4.0 Hz, J' = 3.6 Hz, 2H, ArH), 7.37 (dd, J = 4.0 Hz, J' = 1.2 Hz, 2H, ArH), 7.39 (dd, J = 3.6 Hz, J' = 1.2 Hz, 2H, ArH), 7.65 (s, 2H, ArH), and 7.75 (s, 2H, ArH); ^{13}C NMR δ 118.98, 122.53, 125.98, 126.02, 126.19, 127.83, 130.97, 131.28, 135.37, and 136.55; MS *m/z* 378 (M^+). Found: C, 63.47; H, 2.60%. Calcd for $C_{20}H_{10}S_4$: C, 63.47; H, 2.64%.

5,5′-Dibromo-4,4′-bis(bromomethyl)-2,2′-bis(dibromomethyl)-3,3′-bithiophene (31). A mixture of **30** (11.4 g, 30 mmol) and NBS (38.4 g, 0.216 mol) in carbon tetrachloride (300 mL) was refluxed for 5 h under irradiation of a sunlamp. After cooling, resulting succinimide was filtered off, and the filtrate was concentrated in vacuo to give an oily residue, which was treated with a small amount of acetone to afford a white powder of **31** (21.3 g, 83%). Recrystallization from carbon tetrachloride gave an analytically pure sample of **31** as colorless crystals: mp 196–198 °C; ^{1}H NMR (60 MHz) δ 4.16 (br s, 4H, CH_2), and 6.44 (s, 2H,CH); ^{13}C NMR δ 24.71, 29.71, 119.23, 127.24, 136.00, and 147.61. Anal. Calcd for $C_{12}H_6S_2Br_8$: C, 16.89; H, 0.71%. Found: C, 16.80 H, 0.68%.

5,5′-Dibromo-4,4′-bis(bromomethyl)-3,3′-bithiophene-2,2′-dicarbardehyde (32). To a solution of **31** (17.1 g, 20 mmol) in dioxane (300 mL) was added diluted sulfuric acid (mixed 95 mL of conc. H_2SO_4 with 140 mL of water); the resulting mixture was refluxed for 1.5 h. After cooling, the mixture was poured into 400 mL of water, and the resulting precipitate was collected by filtration and dried in vacuo to afford crude **32** as a pale-yellow solid (10.5 g, 95%). Recrystallization from chloroform gave an analyti-

cally pure sample of **32** as a white powder: mp 185–186 °C; ^{1}H NMR (60 MHz) δ 4.23 (br s, 4H, CH_2) and 9.57 (s, 2H, CHO); ^{13}C NMR δ 23.16, 126.60, 138.08, 138.71, 142.85, and 180.59; IR 2985 and 1681 cm^{-1} (CHO); MS *m*/*z* 566 (M^+). Found: C, 25.42 H, 1.02%. Calcd for $C_{12}H_6O_2S_2Br_4$: C, 25.47; H, 1.07%.

Tetramethyl 5,5′-Dibromo-2,2′-diformyl-3,3′-bithiophene-4,4′-diylbis(methylphosphonate) (33). A mixture of **32** (600 mg, 1.06 mmol) and trimethyl phosphite (10 mL) was refluxed for 2 h. After excess trimethyl phosphite was distilled out in vacuo, the residue was purified with GPC to give pure **33** as a colorless oil (650 mg, quant.): ^{1}H NMR (60 MHz) δ 2.80 (dd, J_{HCH} = 15.0 Hz, J_{PCH} =24.5 Hz, 2H, CH_2), 3.15 (dd, J_{HCH} = 15.0 Hz, J_{PCH} = 24.5 Hz, 2H, CH_2), 3.58 (d, J_{POCH} = 11.0 Hz, CH_3, 6H), 3.66 (d, J_{POCH} = 11.0 Hz, CH_3, 6H), and 9.57 (s, 2H, CHO); ^{13}C NMR δ 25.22, 26.65, 52.51, 123.76, 132.68, 138.84, 143.16, and 181.38; IR (neat) 2851, 1668 (CHO), 1253 (P=O), 1055, and 1028 (P–O) cm^{-1}. Found: C, 30.75 H, 2.86%. Calcd for $C_{16}H_{18}O_8P_2S_2Br_2$: C, 30.79; H, 2.91%.

2,6-Dibromonaphtho[1,8-*bc*:5,4-*b′c′*]dithiophene (34). To a solution of **33** (1.04 g, 1.66 mmol) in DMF (50 mL) was added sodium methoxide prepared in situ from sodium (80 mg, 3.47 mmol) and dry methanol (20 mL) at RT. The resulting green precipitate (230 mg) was collected by filtration and dried. The crude material was recrystallized from carbon disulfide and hexane using activated charcoal powder as a decoloring agent to give golden needles of **34** (160 mg, 26%): mp 102 °C (melt with decomposition in a sealed tube); ^{1}H NMR (CS_2–$CDCl_3$, 400 MHz) δ 7.34 (d, J = 9.25 Hz, 2H, ArH) and 7.62 (d, J = 9.25 Hz, 2H, ArH); ^{13}C NMR (CS_2–$CDCl_3$) δ 107.17, 117.06, 121.52, 129.95, 132.05, and 132.13; MS *m*/*z* 370, 372, and 374 (M^+). Found: C, 38.78 H, 1.14%. Calcd for $C_{12}H_6S_2Br_2$: C, 38.73; H, 1.08%.

Naphtho[1,8-*bc*:5,4-*b′c′*]dithiophene (10). To a well-stirred solution of **34** (50 mg, 0.13 mmol) in THF (20 mL) at −78 °C, butyllithium (0.17 mL, 1.6 M hexane solution, 0.27 mmol) was added, and the temperature was kept for 2.5 h with stirring. The resulting dilithiated species was quenched by slowly adding degassed distilled water (5 mL), and the mixture was allowed to warm to RT. The work-up operations described below were carried out under a nitrogen atmosphere. To the resulting mixture was successively added 5 mL of water, 3 mL of saturated ammonium chloride aqueous solution, and 20 mL of carbon disulfide. The aqueous layer was decanted off, and the organic layer was washed with degassed water and dried ($MgSO_4$). Concentration of the solution under reduced pressure at −30 °C afforded yellow crystals of **10** (19 mg, 61%), which were washed with cold methanol and collected by filtration: mp 93 °C (melt with decomposition in a sealed tube); ^{1}H NMR ($CDCl_3$–CS_2, 400 MHz) δ 7.47 (d, J = 9.2 Hz, 2H, ArH), 7.61 (s, 2H, ArH), and 7.65 (d, J = 9.2 Hz, 2H, ArH); ^{13}C NMR ($CDCl_3$–CS_2) δ 116.9, 118.9, 121.6, 129.6, 132.4, and 133.7; HRMS *m*/*z* 213.9911 (M^+) (Calcd for $C_{12}H_6S_2$: 213.9918). Found: C, 66.77; H, 2.92%. Calcd for $C_{12}H_6S_2$: C, 67.25; H, 2.82%.

2,6-Dimethynaphtho[1,8-*bc*:5,4-*b′c′*]dithiophene (11). The dilithiated **34** generated as described above was quenched with an excess amount of methyl iodide to give **11** as an ocherous powder (60% yield): mp 145 °C (melt with decomposition in a sealed tube); ^{1}H NMR (400 MHz) δ 2.87 (s, 6H, CH_3), 7.23 (d, J = 9.3 Hz, 2H, ArH), and 7.47 (d, J = 9.3 Hz, 2H, ArH); ^{13}C NMR δ 13.26, 115.73, 120.19, 126.45, 130.00, 130.73, and 134.56; MS *m*/*z* 242 (M^+). Found: C, 66.11; H, 4.18%. Calcd for $C_{14}H_{10}S_2$: C, 69.38; H, 4.16%.

2,6-Bis(methythio)naphtho[1,8-*bc*:5,4-*b′c′*]dithiophene (12). The dilithiated **34** generated as described above was quenched with an excess amount of dimethyl disulfide to give **12** as an ocherous powder (71% yield): mp 196 °C (melt with decomposition in a sealed tube); ^{1}H NMR (400 MHz) δ 2.57 (s, 6H, CH_3), 7.57 (d, J = 9.3 Hz, 2H, ArH), and 7.63 (d, J = 9.3 Hz, 2H, ArH); ^{13}C NMR δ 23.14, 117.76, 121.13, 129.64, 131.60, 133.43, and 134.74; MS *m*/*z* 306 (M^+). Found: C, 54.75; H, 3.17%. Calcd for $C_{14}H_{10}S_4$: C, 54.86; H, 3.29%.

2,6-Di(2-thienyl)naphtho[1,8-*bc*:5,4-*b′c′*]dithiophene (13). Compound **13** was obtained in 60% yield from **34** in a similar manner as described for the synthesis of **9**: purple needles from chloroform–hexane; mp 245–247 °C; ^{1}H NMR (400 MHz) δ 7.11 (dd, J = 4.8 Hz, J' = 3.6 Hz, 2H, ArH), 7.34 (dd, J = 4.8 Hz, J' = 0.8 Hz, 2H, ArH), 7.42 (dd, J = 3.6 Hz, J' = 0.8 Hz, 2H, ArH), 7.70 (d, J = 9.3 Hz, 2H, ArH), and 7.84 (d, J = 9.3 Hz, 2H, ArH); ^{13}C NMR δ 118.64, 121.54, 124.83, 125.20, 126.19, 127.90, 128.29, 128.64, 129.62, 134.86, and 137.06; MS *m*/*z* 378 (M^+). Found: C, 63.23; H, 2.64%. Calcd for $C_{20}H_{10}S_4$: C, 63.47; H, 2.64%.

Molecular Complexes and Radical Cation Salts. The iodine and DDQ complexes were prepared by a conventional mixing method using acetonitrile as a solvent. All of the radical cation salts were prepared by electrocrystallization under galvanostatic conditions (2.0–8.0 μA) in THF or acetonitrile containing *n*-$Bu_4N^+X^-$ (X^- = BF_4^-, ClO_4^-, PF_6^-, and I_3^-) as the supporting electrolyte.

Crystal Structure Determinations. A Rigaku AFC-6S diffractometer with graphite-monochromated Cu $K\alpha$ radiation (λ = 1.548 Å) was used, and data were collected at room temperature for the crystal of **6**. The intensities were measured from continuous ω–2θ scans, and were corrected for Lorenz polarization effects. The structure was solved by direct methods. All non-hydrogen atoms were refined by a full-matrix least-squares technique with anisotropic temperature factors.

Crystal data for **6**: $C_{12}H_6S_2$, M_r = 214.31, *monoclinic*, space group $P2_1$, a = 7.837(1) Å, b = 4.128(1) Å, c = 14.035(4) Å, β = 93.35(6)°, V = 453.2(2) Å^3, Z = 2, D_{calcd} = 1.571 g cm^{-3}, R = 0.042. The crystallographic data for **6** was deposited in the Cambridge Crystallographic Data Centre under reference code HAHCOI as a part of a previous communication.[15a]

A Rigaku RAXIS-RAPID Imaging Plate diffractometer with graphite-monochromated Mo $K\alpha$ radiation (λ = 0.7107 Å) was used, and data were collected at room temperature for the crystal of **13**. The camera radius was 127.40 mm, and readout was performed in the 0.100 mm pixel mode. All of the data were corrected for Lorenz and polarization effects. The structure was solved by direct methods. All non-hydrogen atoms were refined anisotropically by a full-matrix least-squares technique. Hydrogen atoms were included, but not refined.

Crystal data for **13**: $C_{20}H_{10}S_4$, M_r = 378.54, *monoclinic*, space group $P2_1/c$, a = 13.333(1), b = 3.9332(7), c = 15.258(1) Å, β = 97.031(7)°, V = 794.1(2) Å^3, Z = 2, D_{calcd} = 1.583 g cm^{-3}, R = 0.064. The crystallographic data for **13** (excluding structure factors) has been deposited in the Cambridge Crystallographic Data Centre as supplementary publication no. CCDC 178734. Copies of the data can be obtained free of charge on application to The Director, CCDC, 12 Union Road, Cambridge CB2 1EZ, UK (fax: Int. code +(1223) 336-033; e-mail: deposit@chemcrys.cam.ac.uk).

This work was partially supported by Grants-in-Aid for Scientific Research from the Ministry of Education, Culture, Sports, Science and Technology. The authors are very grateful to Prof. Y. Yamashita (Tokyo Institute of Technology) and Dr. C. Kitamura (Himeji Institute of Technology) for experimental guidance.

References

1 For reviews on organic conductors based on sulfur-containing aromatics, see a) K. Nakasuji, *Pure Appl. Chem.*, **62**, 477 (1990). b) T. Otsubo, *Synlett*, **1997**, 544.

2 a) T. Noda, H. Ogawa, N. Noma, and Y. Shirota, *Adv. Mater.*, **9**, 720 (1997). b) Y. Shirota, *J. Mat. Chem.*, **10**, 1 (2000). c) U. Mitschke and P. Bäuerle, *J. Mat. Chem.*, **10**, 1471 (2000).

3 R. J. Mortimer, *Chem. Soc. Rev.*, **26**, 147 (1997).

4 a) J. G. Laquindanum, H. E. Katz, and A. J. Lovinger, *J. Am. Chem. Soc.*, **120**, 664 (1998). b) X.-C. Li, H. Sirringhaus, F. Garnier, A. B. Holmes, S. C. Moratti, N. Feeder, W. Clegg, S. J. Teat, and R. H. Friend, *J. Am. Chem. Soc.*, **120**, 2206 (1998). c) H. Meng, Z. Bao, A. J. Lovinger, B.-C. Wang, and A. M. Mujsce, *J. Am. Chem. Soc.*, **123**, 9214 (2001); H. E. Katz, Z. Bao, and S. L. Gilat, *Acc. Chem. Res.*, **34**, 359 (2001).

5 a) H. Akamatu, H. Inokuchi, and Y. Matsunaga, *Nature (London)*, **173**, 168 (1954). b) H. Akamatu, H. Inokuchi, and Y. Matsunaga, *Bull. Chem. Soc. Jpn.*, **29**, 213 (1956). c) M. M. Labes, R. Sehr, and M. Bose, *J. Chem. Phys.*, **33**, 868 (1960). d) J. Kommandeur and F. R. Hall, *J. Chem. Phys.*, **34**, 129 (1961). e) C. Kröhnke, V. Enkelmann, and G. Wegner, *Angew. Chem., Int. Ed. Engl.*, **19**, 912 (1980).

6 F. Wudl, R. C. Haddon, E. T. Zellers, and F. B. Bramwell, *J. Org. Chem.*, **44**, 2491 (1979).

7 a) Y. Kono, H. Miyamoto, Y. Aso, T. Otsubo, F. Ogura, T. Tanaka, and M. Sawada, *Angew. Chem., Int. Ed. Engl.*, **28**, 1222 (1989). b) T. Otsubo, Y. Kono, N. Hozo, H. Miyamoto, Y. Aso, F. Ogura, T. Tanaka, and M. Sawada, *Bull. Chem. Soc. Jpn.*, **66**, 2033 (1993).

8 D. J. Sandman and G. P. Ceasar, *Isr. J. Chem.*, **27**, 293 (1986).

9 Y. Tominaga, M. L. Lee, and R. N. Castle, *J. Heterocyclic Chem.*, **18**, 977 (1981).

10 MO calculations were performed by using the MOPAC Ver. 6.0 program package with an MNDO method.

11 For excellent reviews on low bandgap polymers, see: a) J. Roncali, *Chem. Rev.*, **97**, 173 (1997). b) M. Pomerantz, "Handbook of conducting polymers, 2nd ed," ed by T. A. Skotheim, R. L. Elsenbaumer, and J. R. Reynolds, Marcel Dekker, New York (1998), Chapter 11, pp. 277–309.

12 a) F. Wudl, M. Kobayashi, and A. J. Heeger, *J. Org. Chem.*, **49**, 3382 (1984). b) M. Kobayashi, N. Boysel, F. Wudl, and A. J. Heeger, *J. Chem. Phys.*, **82**, 5717 (1985).

13 R. H. Mitchell and V. Boekelheide, *J. Am. Chem. Soc.*, **92**, 3510 (1970); **96**, 1547 (1974).

14 K. Watanabe, Y. Aso, T. Otsubo, and F. Ogura, *Chem. Lett.*, **1992**, 1233.

15 The preliminary synthetic studies of naphthodithiophenes were reported in the following communications: a) K. Takimiya, F. Yashiki, Y. Aso, T. Otsubo, and F. Ogura, *Chem. Lett.*, **1993**, 365. b) K. Takimiya, T. Otsubo, and F. Ogura, *J. Chem. Soc., Chem. Commun.*, **1994**, 1859.

16 J. Sicé, *J. Org. Chem.*, **19**, 70 (1954).

17 T. Mukaiyama, T. Sato, and J. Hanna, *Chem. Lett.*, **1973**, 1041.

18 R. M. Kellogg, M. B. Groen, and H. Wynberg, *J. Org. Chem.*, **32**, 3093 (1967).

19 A. Moradpour, *J. Chem. Soc., Perkin Trans. 1*, **1993**, 7.

20 E. Wiklund and R. Håkansson, *Chem. Scr.*, **3**, 220 (1973).

21 B. Back, D. Christensen, L. Hansen-Nygaard, and J. Rastrup-Andersen, *J. Mol. Spec.*, **7**, 58 (1961).

22 R. Allmann, *Z. Kristallogr.*, **132**, 129 (1970).

23 The conductivity was measured on a compressed pellet of a pristine polymer sample in heavily doped state.

24 A. Ottenberg, R. L. Brandon, and M. E. Browne, *Nature (London)*, **201**, 1119 (1964).

25 T. Ishiguro, K. Yamaji, and G. Saito, "Organic Superconductors," Springer-Verlag, Berlin (1997).

26 a) J. P. Ferraris and T. L. Lambert, *J. Chem. Soc., Chem. Commun.*, **1991**, 1268. b) M. Pomerantz, B. Chaloner-Gill, L. O. Harding, J. J. Tseng, and W. J. Pomerentz, *J. Chem. Soc., Chem. Commun.*, **1992**, 1672. c) M. V. Lakshmikantham, D. Lorcy, C. Scordilis-Kelley, X.-L. Wu, J. P. Parakka, R. M. Metzger, and M. P. Cava, *Adv. Mater.*, **5**, 723 (1993). d) G. King and S. J. Higgins, *J. Mater. Chem.*, **5**, 447 (1995). e) J. Kastner, H. Kuzmany, D. Vegh, M. Londl, L. Cuff, and M. Kertesz, *Synth. Met.*, **69**, 593 (1995).

27 a) E. E. Havinga, W. ten Hoeve, and H. Wynberg, *Polym. Bull.*, **29**, 119 (1992). b) E. E. Havinga, W. ten Hoeve, and H. Wynberg, *Synth. Met.*, **55-57**, 299 (1993). c) E. E. Havinga, A. Pomp, W. ten Hoeve, and H. Wynberg, *Synth. Met.*, **69**, 581 (1995). d) S. Tanaka and Y. Yamashita, *Synth. Met.*, **55-57**, 1251 (1993). e) S. Tanaka and Y. Yamashita, *Synth. Met.*, **69**, 599 (1995). f) M. Karikomi, C. Kitamura, S. Tanaka, and Y. Yamashita, *J. Am. Chem. Soc.*, **117**, 6791 (1995). g) C. Kitamura, S. Tanaka, and Y. Yamashita, *Chem. Lett.*, **1996**, 63. h) C. Kitamura, S. Tanaka, and Y. Yamashita, *Chem. Mater.*, **8**, 570 (1996). i) C. L. Kean and P. G. Pickup, *Chem. Commun.*, **2001**, 815.